読影判定法

１．　脳局所集積の視覚的判定

アルツハイマー病で特異的な集積を呈する大脳領域、すなわち、節前部・後部帯状回、前頭葉、側頭葉外側、頭頂葉外側、線条体への集積を、左右別に 3 段階で判定する。

Ａ：集積あり（○）　白質への集積を明らかに上回る集積が 1 脳回を越える広がりをもって認められる。ピンポイントの集積は採用しない。線条体の場合は視床や脳幹部、小脳髄質よりも明瞭に高い集積が認められる場合をとる。

Ｂ：集積の疑い（△）　白質への集積と同等か僅かに上回る集積が 1 脳回を越える広がりをもって認められる。1 脳回よりも狭いがピンポイントで高い集積があればここに含める。集積は白質皮質の境界を越え、皮質辺縁にまで及ぶものをとる。線条体の場合、周辺の白質と区別できるが視床や脳幹部、小脳髄質を越えない程度の集積の場合ここに含める。

Ｃ：集積なし（×）　白質への集積よりも低い場合。ただし、線条体の場合は周囲白質と区別が付かず、concentric な集積を認めなければここに含める。
上記 5 部位以外に集積があれば、別途記載する。

２．　全体判定

上記 5 部位のうち皮質 4 部位への集積のみに基づいて判定する。皮質 4 部位への集積が 1 部位以上で認められた場合（○が一つでもあれば）集積あり（陽性）と判定する。同皮質部位での判定に疑い（△）がある場合は疑いとする。部位への集積が認められない場合（全て×）は、集積なしと判定する。すなわち、線条体およびその他の部位への集積は全体判定には勘案しない。

判定についての留意点

FDG-PET の読影に用いる Silverman によるパターン分類は、背景となる病態が変性型であるか否か、変性型であるとすれば AD であるかどうかという診断的意義を背景とした判断であるのに対し、PiB-PET の読影は、集積の有無のみに着目し、その診断的意義の解釈は行わない。（コメントに書くことは差し支えない）。

J-ADNI PiB PET 中央読影実施要領

2009 年 7 月 28 日

目的

J-ADNI ではアミロイド PET の検査結果を被験者の希望により開示できることとなっている。開示指針にもとづいて担当医師が被験者に結果を開示するための検査結果報告書を提供することと、合わせてアミロイド PET の視覚的読影方法を確立し、各グループの陽性率等を検討することを目的として、アミロイド PET の中央読影を実施する。本実施要領では PiB-PET の実施方法について定める。

読影画像の準備

J-ADNI の各プロトコル及びマニュアルに従って撮影され、PET QC チームで品質保証された画像を読影に供する。PiB 投与 50-70 分の加算画像（位置補正、standard voxel 処理済み）と、これに 4 mm FWHM の Gaussian filter によりノイズを低減した画像を作成し、1 例についてこの 2 画像を DICOM 書式に出力して、読影者に提供する

読影者

3 名の読影者（J-ADNI FDG-PET 中央読影と共通）が個々の環境で、ブラウザーを用いて画像を表示し、読影指針に基づいて読影する。表示はカラースケール、モノクロスケールの何れでも可。

読影指針

別紙参照。

結果の入力

ファイルメーカープロで作成した結果入力用ファイル（読影画像と共に読影者に配付）に、読影結果を入力する。入力したファイルは、読影終了後、PET QC チームに返送する。

集計とコンセンサス読影

3 名の読影者による読影結果を集計し、全体判定が一致しない場合、コンセンサス読影により判定を決定する。局所集積に関しては 3 名の結果を平均する。

読影報告書

コンセンサス読影を経た読影結果を、報告書として発行する。報告書には、被験者を同定できる情報、撮影日、検査法とともに、全体判定と、局所集積の判定（平均）を記載する。また、判定により、被験者への説明の例を、開示指針にもとづいて提示する。

参考画像と解説

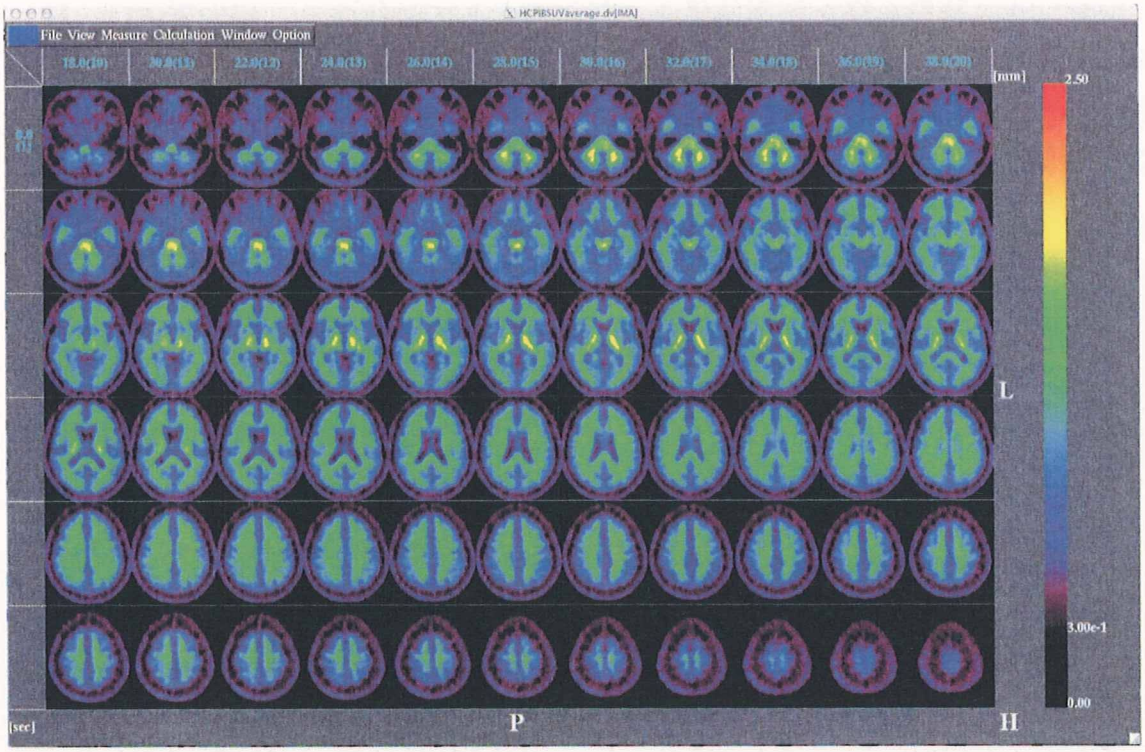

図１　健常者における PiB 後期 SUVR 画像の平均イメージ　特徴が分かりやすいように、ここでは 50-70 分の加算画像を小脳皮質への集積で基準化し、7 名分を平均した画像を示す。白質に比較的均一な集積があり、これを基準にしてみると、大脳皮質、小脳皮質への集積は、白質よりも低いレベルにあることが分かる。また、視床、脳幹部（特に橋底部）、小脳髄質への集積は、大脳白質よりもやや高い。健常人でも前頭葉の灰白質は他部位の灰白質に比べ集積はやや高めで、画像の分解能によっては白質よりも灰白質への集積が低いことが分かりにくい傾向があるが、皮質の辺縁に至るまで、白質と同等あるいはそれ以上の集積が 1 脳回を越えた広がりを持って明瞭に存在しなければ、集積疑いあるいは陽性とは判定しない。

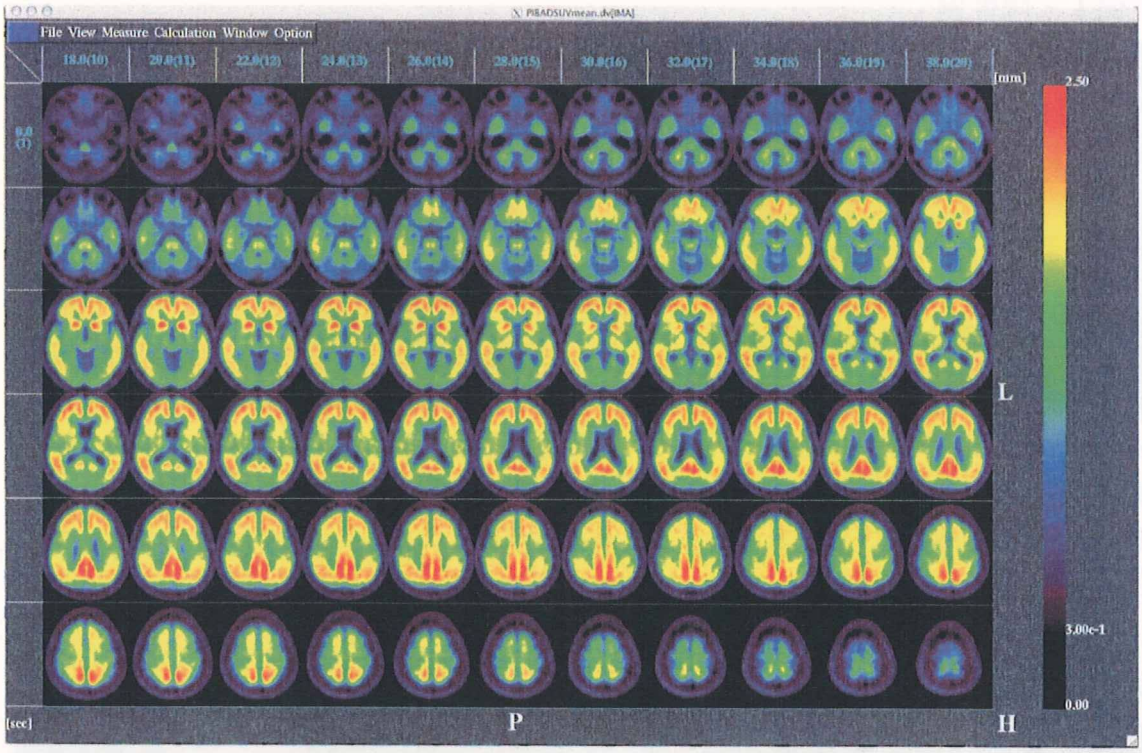

図２　アルツハイマー病患者における PiB 後期 SUVR 画像の平均イメージ　健常者と同様で、50-70 分の加算画像を小脳皮質への集積で基準化したもので、20 例分を平均した画像を示す。大脳白質のレベルを超える集積が連合野皮質の広範な領域で認められる。楔前部・後部帯状回領域への集積が最も高く、次いで前頭葉、側頭頭頂葉外側皮質が高い。また線条体（特に腹側部）にも大脳白質レベルを超えた集積が認められる。後頭葉一次視覚野、中心前後回への集積は相対的に目立たない（しかし、健常者よりは高い）。側頭葉内側部（海馬、扁桃核）や島皮質への集積も比較的目立たない。脳室周囲の白質への集積、橋への集積、小脳皮質への集積は健常者と比べて有意な変化はないといわれているので、読影の際に目安とすることが出来る。

症例１：陽性例

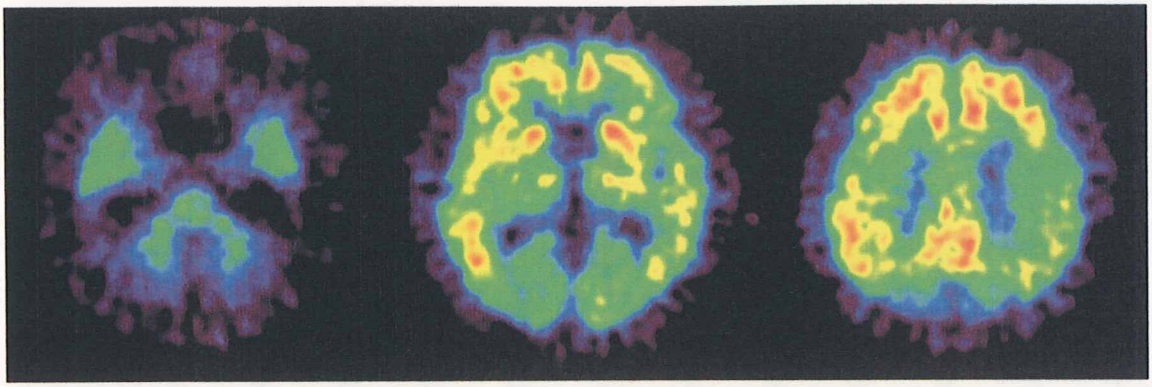

AD 典型例。脳室周囲の白質レベルと比べ明らかに高い大脳皮質への集積が楔前部、前頭葉、側頭葉、頭頂葉に見られる。線条体への集積もあ認められる。中央スライスの後頭葉は白質と同等レベルの集積ありとみなせる（△）。右スライスの後頭葉上部は集積がない。

症例２：陰性例

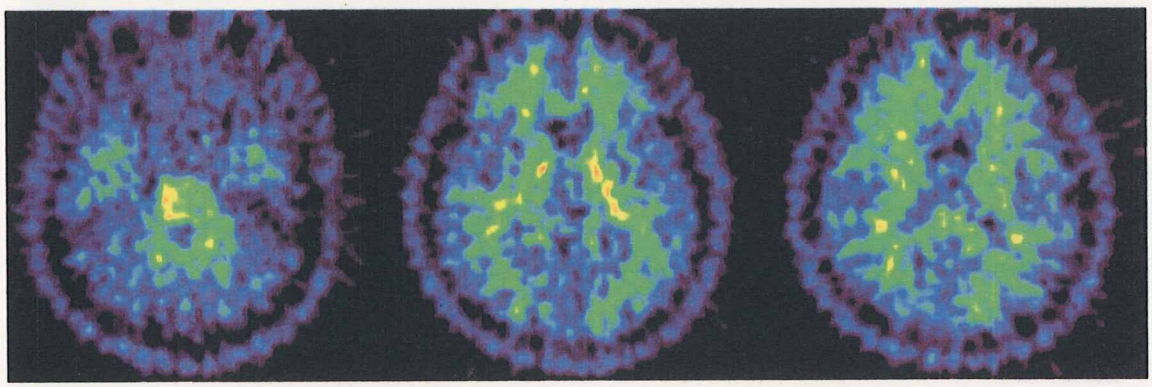

画像の最大値を自動的にマップし表示する設定のブラウザだと、白質や視床、脳幹部が高値に対応する色調で表示されることがあり、紛らわしい。まず、大脳皮質に白質を越える集積はないことを確認する。右スライスで、前頭葉に白質と同等の集積があるかどうか分かりにくいが、フィルターをかけて解像度を落とした画像を参照すると（下図）、

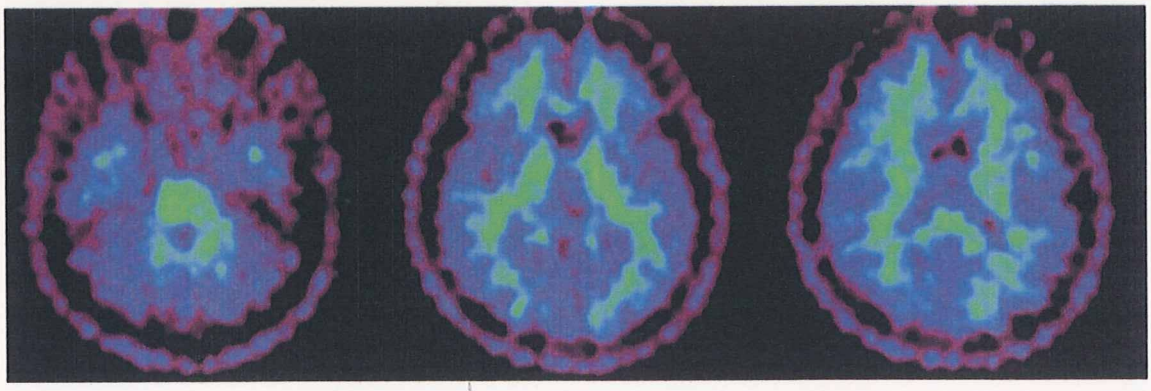

白質皮質の境界を越え、皮質の辺縁まで至る集積はないことが分かる。

症例３：集積疑い例

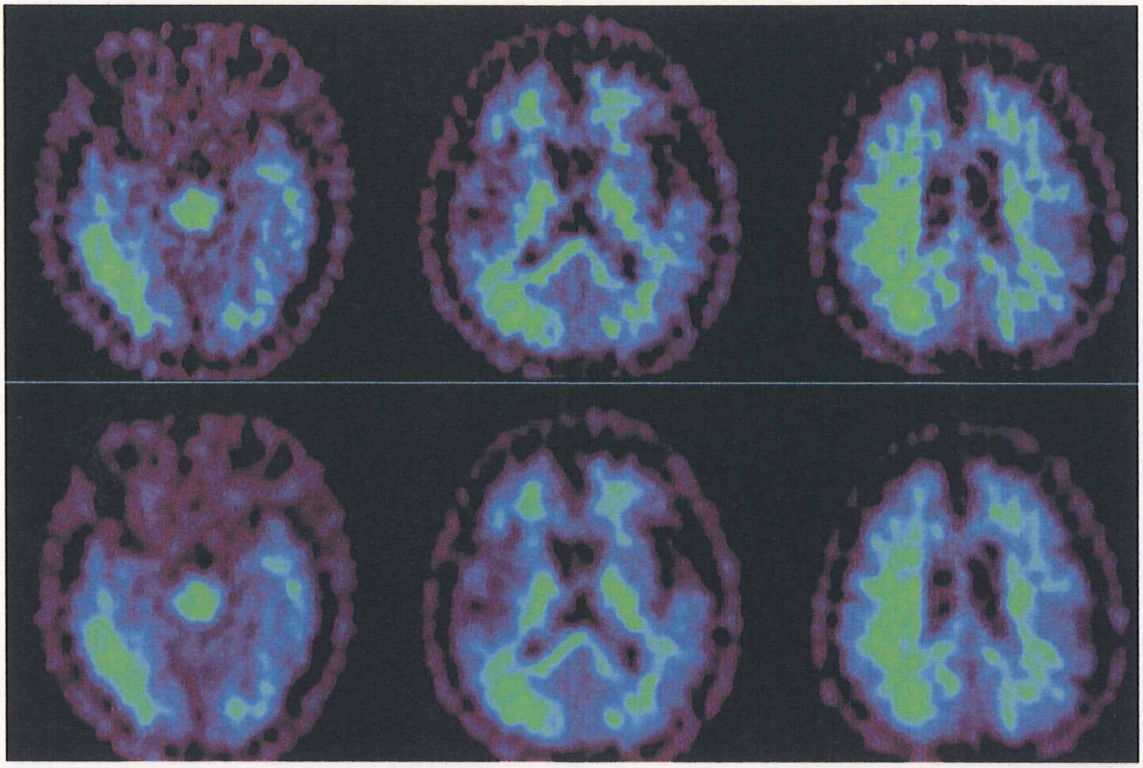

この症例では、右側頭葉から頭頂葉に書けての皮質に、白質への集積を越えないレベルの集積があり、皮質の辺縁に達して、しかも 1 脳回を越えた広がりがある。このような場合は集積疑い（△）と判定する。左右差があり、皮質と白質のコントラストが部位によって異なっているので、分かりやすい。通常集積の余りない後頭葉や中心前後回、側頭葉内側部、小脳皮質も含め、脳全体の皮質が白質と同等の集積があるように見える場合は、画像の解像度の問題である可能性があるので、判定は慎重に行う。PiB の集積は全脳の皮質に均一に増加することは経験上ないので、集積あり（○）あるいは疑い（△）の判定ができるのは、局所集積としての特徴を有する場合である。

Ⅳ. 研究成果の刊行に関する一覧表

研究成果の刊行に関する一覧表

1. 英文原著・症例報告

著者名	論文題名	雑誌名	巻	頁	出版年
Miyamoto T, Orimo S, Miyamoto M, Hirata K, Adachi T, Hattori R, Suzuki M, Ishii K.	Follow-up PET studies in case of idiopathic REM sleep behavior disorder.	Sleep Med	10(1)	100-101	2010
Kambe T, Motoi Y, Ishii K, Hattori N.	Posterior cortical atrophy with [^{11}C]Pittsburgh compound B accumulation in the primary visual cortex.	J Neurol.	in press	オンライン出版 2009 Nov 14. DOI: 10.1007/s00415-009-5377-y	2009
Ishibashi K, Ishii K, Oda K, Mizusawa H, Ishiwata K.	Competition between ^{11}C-raclopride and dendogeneous dopamine in Parkinson's disease.	Nucl Med Commun.	in press	オンライン出版 2009 Dec 3. DOI: 10.1097/MNM.0b013e328333e3cb	2009
Emot H, Suzuki Y, Wakakura M, Horie C, Kiyosawa M, Mochizuki M, Kawasaki K, Oda K, Ishiwata K, Ishii K.	Photophobia in essential blepharospasm - A positron emission tomographic study.	Mov Disorders.	in press	オンライン出版 2009 Dec 11. DOI: 10.1002/mds.29916	2009
Ishibashi K, Kanemaru K, Saito Y, Murayama S, Oda K, Ishiwata K, Mizusawa H, Ishii K.	Cerebrospinal fluid metabolite and nigrostriatal dopaminergic function in Parkinson's disease	Acta Neurol Scand.	in press	オンライン出版 2009 Nov 30. DOI: 10.1111/j.1600-0404.2009.01255.x	2009
Ishikawa M, Sakata M, Ishii K, Kimura Y, Oda K, Toyohara J, Wu J, Ishiwata K, Iyo M, Hashimoto K.	High occupancy of σ1 receptors in the human brain after single oral administration of donepezil: a positron emission tomography study using [^{11}C]SA4503	Int J Neuropsychopharmacol.	12(8)	1127-1131	2009
Ishibashi K, Saito Y, Murayama S, Kanemaru K, Oda K, Ishiwata K, Mizusawa H, Ishii K.	Validation of cardiac ^{123}I-MIBG scintigraphy in patients with Parkinson's disease who were diagnosed with dopamine PET.	Eur J Nucl Med Mol Imaging	37(1)	3-11	2010
Nishioka K, Ross OA, Ishii K, Kachergus JM, Ishiwata K, Kitagawa M, Kono S, Obi T, Mizoguchi K, Inoue Y, Imai H, Takanashi M, Mizuno Y, Farrer MJ, Hattori N.	Expanding the clinical phenotype of SNCA duplication carriers.	Mov Disorders	24(12)	1811-1819	2009
Ishibashi K, Ishii K, Oda K, Kawasaki K, Mizusawa H, and Ishiwata K.	Regional analysis of age-related decline in dopamine transporters and dopamine D_2-like receptors in human striatum.	Synaps	63(4)	282-290	2009
Shimada H, Hirano S, Shinotoh H, Aotsuka A, Sato K, Tanaka N, Ota T, Asahina M, Fukushi K, Kuwabara S, Hattori T, Suhara T, Irie T.	Mapping of brain acetylcholinesterase alterations in Lewy body disease by PET.	Neurology	73	273-278	2009
Hirano S, Asahina M, Uchida Y, Shimada H, Sakakibara R, Shinotoh H, Hattori T.	Reduced perfusion in the anterior cingulate cortex of patients with pure autonomic failure: an ^{123}I-IMP SPECT study.	J Neurol Neurosurg Psychiatry.	80	1053-55	2009

Ota T, Shinotoh H, Fukushi K, Kikuchi T, Sato K, Tanaka N, Shimada H, Hirano S, Miyoshi M, Arai H, Suhara T, Irie T.	Estimation of Plasma IC_{50} of Donepezil for Cerebral Acetylcholinesterase Inhibition in Patients With Alzheimer Disease Using Positron Emission Tomography.	Clin Neuropharmacol	in press	オンライン出版 2009 Nov 21. DOI: 10.1097/WNF.0b013e3181c71be9	2009
Okamura N, Shiga Y, Furumoto S, Tashiro M, Tsuboi Y, Furukawa K, Yanai K, Iwata R, Arai H, Kudo Y, Itoyama Y, Doh-Ura K.	In vivo detection of prion amyloid plaques using [^{11}C]BF-227 PET.	Eur J Nucl Med Mol Imaging.	in press	オンライン出版 2009 Dec 17. DOI: 10.1007/s00259-009-1314-7	2009
Furukawa K, Okamura N, Tashiro M, Waragai M, Furumoto S, Iwata R, Yanai K, Kudo Y, Arai H.	Amyloid PET in mild cognitive impairment and Alzheimer's disease with BF-227: comparison to FDG-PET.	J Neurol.	in press	オンライン出版 2009 Nov 28. DOI: 10.1007/s00415-009-5396-8	2009
Waragai M, Okamura N, Furukawa K, Tashiro M, Furumoto S, Funaki Y, Kato M, Iwata R, Yanai K, Kudo Y, Arai H.	Comparison study of amyloid PET and voxel-based morphometry analysis in mild cognitive impairment and Alzheimer's disease.	Neurol Sci.	285	100-108	2009
Hiraoka K, Okamura N, Funaki Y, Watanuki S, Tashiro M, Kato M, Hayashi A, Hosokai Y, Yamasaki H, Fujii T, Mori E, Yanai K, Watabe H.	Quantitative analysis of donepezil binding to acetylcholinesterase using positron emission tomography and [5-^{11}C-methoxy]donepezil.	Neuroimage.	46	616-623	2009
Ishii H, Ishikawa H, Meguro K, Tashiro M, Yamaguchi S.	Decreased cortical glucose metabolism in converters from CDR 0.5 to Alzheimer's disease in a community: the Osaki-Tajiri Project.	Int Psychogeriatr.	21	148-156	2009
Ouchi Y, Yoshikawa E, Futatsubashi M, Yagi S, Ueki T, Nakamura K.	Altered brain serotonin transporter and associated glucose metabolism in Alzheimer's disease	J Nucl Med	50	1260-1266	2009

2. 英文単行本

著者名	論文題名	書名	編集者名	出版社名	出版地	頁	出版年
Tashiro M, Fujitmoto T, Okamura N, Iwata R and Yanai K.	Molecular and functional imaging for drug development and elucidation of disease mechanisms.	Molecular Imaging for Integrated Medical Therapy.	Nagara TAMAKI and Yuji KUGE	Springer	Japan	222-234	2010

3. 邦文総説

著者名	論文題名	雑誌名	巻	頁	出版年
石井賢二	認知症の新しい画像診断法	Modern Physician	30(1)	58-61	2010
石井賢二	PETによるアミロイドイメージングを用いたAD診断	Med Imag Tech	28(1)	26-30	2010
石井賢二	[^{11}C]フルマゼニルによるGABAA受容体PETイメージング	RADIOISOTOPES	59(1)	49-58	2010
石井賢二	軽度認知障害の画像診断	老年精神医学雑誌	20(3)	271-279	2009
篠遠仁	認知症の診断-この10年とこれから- 機能画像の進歩	老年精神	21	42-48	2010
篠遠仁	PET, SPECT -パーキンソン病における治療効果の評価-	日本臨床	67	228-232	2009
篠遠仁	アミロイドイメージングの進歩	Clinician	56	44-50	2009

伊藤健吾，加藤隆司	FDG-PETによるアルツハイマー病の早期診断	Dementia Japan	23	14-21	2009
伊藤健吾，加藤隆司	認知症の診断と根本治療薬の開発に貢献するPETイメージング	日本神経精神薬理雑誌	29	153-160	2009

4. 邦文単行本

著者名	論文題名	書名	編集者名	出版社名	出版地	頁	出版年
石井賢二	アミロイドイメージング	Annual Review 神経2010	鈴木則弘ほか	中外医学社	東京	57-64	2010

Ⅴ. 研究成果の刊行物・別刷

Sleep Medicine 11 (2010) 100–101

Contents lists available at ScienceDirect

Sleep Medicine

journal homepage: www.elsevier.com/locate/sleep

Introduction to Images in Sleep Medicine

This section is intended to tap into a relatively unique feature of sleep science: images with great educational and conceptual content (e.g., electroencephalograms, electromyograms, polysomnograms, portable devices, actigrams, scans including functional images, pathology specimens, brain slice preparations, fluorescent microscopy and other cutting edge techniques). Please see our web site's (http://ees.elsevier.com/sleep/) **Guide for Authors** for instructions. We hope this section will be enriched by the contributions of our colleagues who wish to offer stimulating opportunities for discussion and new insights into the field of sleep.

doi:10.1016/S1389-9457(09)00442-0

Follow-up PET studies in case of idiopathic REM sleep behavior disorder

Tomoyuki Miyamoto [a,*], Satoshi Orimo [b], Masayuki Miyamoto [a], Koichi Hirata [a], Tomoko Adachi [b], Ryo Hattori [b], Masahiko Suzuki [c,d], Kenji Ishii [d]

[a] Department of Neurology, Center of Sleep Medicine, Dokkyo Medical University School of Medicine, Japan
[b] Department of Neurology, Kanto Central Hospital, Japan
[c] Department of Neurology, The Jikei University School of Medicine, Japan
[d] Positron Medical Center, Tokyo Metropolitan Institute of Gerontology, Japan

ARTICLE INFO

Article history:
Received 6 April 2009
Accepted 15 May 2009
Available online 9 July 2009

Keywords:
Idiopathic REM sleep behavior disorder
PET
Cardiac ^{123}I-MIBG scintigraphy
Parkinson's disease
Dementia with Lewy bodies
Neurodegenerative disease

1. Introduction

REM sleep behavior disorder (RBD) is a frequent feature of Parkinson's disease (PD) or dementia with Lewy bodies (DLB) and is characterized by dream-enacting behaviors, unpleasant dreams, and loss of muscle atonia during REM sleep [1]. Progression to PD or DLB has been reported in some patients with idiopathic RBD (iRBD) [1,2]. We followed the present case by PET immediately after development of iRBD and yearly for 2.5 years.

A 73-year-old man presented because of a history of distinct talking and falling out of bed during sleep beginning at around the age of 70 years. He had a history of sleep talk and feeling faint when standing up during the previous 6 years. Mild rigidity was noted in his right wrist and he had a slight frontal gait, but no bradykinesia or tremor. During the head-up tilt test blood pressure was 121/69 mmHg in the supine position and 99/49 mmHg in the upright position. In both the first (at 71 years) and second study (at 73 years), the heart-to-mediastinum (H/M) ratio was reduced (early 1.68, delayed 1.45; early 1.36, delayed 1.12, respectively) in ^{123}I-MIBG cardiac scintigraphy (MIBG) [3]. Polysomnography showed the REM sleep without atonia. RBD was defined according to criteria in the International Classification of Sleep Disorders, second edition.

2. Image analysis

The viability of presynaptic dopaminergic neurons was evaluated by PET with [^{11}C]carbomethoxy flurophenyl tropane (CFT). Activity was calculated using the ratio index [i.e., (target region of interest-cerebellum/cerebellum) and compared with results from healthy control subjects ($n = 6$, ages 57–74).

Activities of the right/left caudate, anterior putamen and posterior putamen of CFT were 3.63/3.70, 3.87/3.75 and 3.35/3.22, respectively, at age 71 one year after RBD onset and 3.27/3.13, 3.41/3.3 and 2.79/2.88, respectively, 2.5 years after the first scan. Rate of decrease (%) of right/left caudate, anterior putamen and posterior putamen per year was 3.95/6.45, 4.83/4.67 and 6.60/4.04, respectively (Fig. 1).

3. Discussion

Nigrostriatal presynaptic dopaminergic function was normal 1 year after diagnosis of iRBD and decreased by 4~6% per year,

* Corresponding author. Address: Dokkyo Medical University School of Medicine, 880 Kitakobayashi Mibu, Tochigi 321-0293, Japan.
E-mail address: miyatomo@dokkyomed.ac.jp (T. Miyamoto).

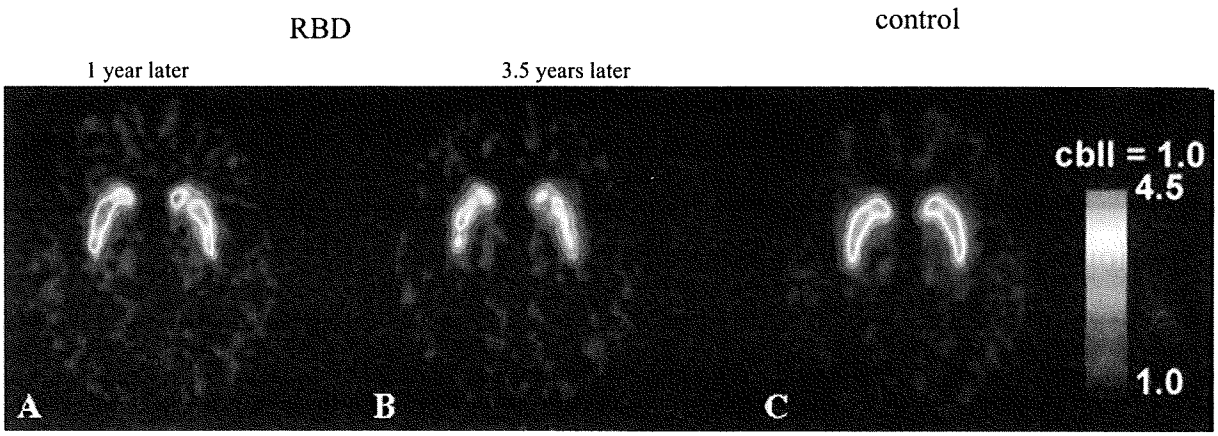

Fig. 1. Images of [^{11}C]carbomethoxy flurophenyl tropane: nigrostrial presynaptic dopaminergic function was almost normal except for a slight decrease in the left posterior putamen at 71 years (A: August 2004) compared with control subject (C), but decreased by 4–6% per year at 2.5 years after the first scan (B: January 2007).

which is similar to that in PD [4]. But reduced cardiac MIBG uptake and orthostatic hypotension had already appeared at the onset of iRBD, indicating that degeneration of non-motor neurons preceded that of motor neurons. We reported that cardiac MIBG uptake is reduced in patients with iRBD, suggesting that the cardiac sympathetic nerve involvement and lesions responsible for iRBD develop during the same period [3].

Few longitudinal published studies have addressed the natural course of iRBD. Eleven of 29 older men (38%) diagnosed with iRBD developed parkinsonian disorders within 3.7 years, and 17 of 26 patients (65.4%) developed the disease within 13 years of diagnosis of iRBD [1]. Twenty-six of 93 cases of iRBD progressed to neurodegenerative disease: 17.7% at 5 years; 40.6% at 10 years; and 52.4% at 12 years [2]. Onset of PD usually begins a few years to a little over a decade after the development of iRBD. Moreover, degeneration of the cardiac sympathetic nerve precedes involvement of nigrostriatal presynaptic dopaminergic function in RBD [5].

References

[1] Gagnon JF, Postuma RB, Mazza S, Doyon J, Montplaisir J. Rapid-eye movement sleep behavior disorder and neurodegenerative diseases. Lancet Neurol 2006;5:424–32.
[2] Postuma RB, Gagnon JF, Vendette M, Fantini ML, Massicotte-Marquez J, Montplaisir J. Quantifying the risk of neurodegenerative disease in idiopathic REM sleep behavior disorder. Neurology 2009;72:1296–300.
[3] Miyamoto T, Miyamoto M, Suzuki K, Nishibayashi M, Iwanami M, Hirata K. ^{123}I-MIBG cardiac scintigraphy provides clues to the underlying neurodegenerative disorder in idiopathic REM sleep behavior disorder. Sleep 2008;31:717–23.
[4] Nurmi E, Bergman J, Eskola O, Solin O, Vahlberg T, Sonninen P, et al. Progression of dopaminergic hypofunction in striatal subregions in Parkinson's disease using [18F]CFT PET. Synapse 2003;48:109–15.
[5] Eisensehr I, Linke R, Tatsch K, Kharraz B, Gildehaus JF, Wetter CT, et al. Increased muscle activity during rapid eye movement sleep correlates with decrease of striatal presynaptic dopamine transporters. IPT and IBZM SPECT imaging in subclinical and clinically manifest idiopathic REM sleep behavior disorder, Parkinson's disease, and controls. Sleep 2003;26:507–12.

doi: 10.1016/j.sleep.2009.05.006

J Neurol
DOI 10.1007/s00415-009-5377-y

LETTER TO THE EDITORS

Posterior cortical atrophy with [^{11}C] Pittsburgh compound B accumulation in the primary visual cortex

Taiki Kambe · Yumiko Motoi · Kenji Ishii · Nobutaka Hattori

Received: 24 August 2009 / Revised: 24 October 2009 / Accepted: 30 October 2009

Sirs,

Posterior cortical atrophy (PCA) is a presenile dementia that presents primarily with signs and symptoms of cortical visual dysfunction [1]. The most common associated pathologic findings of PCA are amyloid plaques and neurofibrillary tangles predominantly affecting the visual association areas [8]. Although [^{11}C] Pittsburgh compound B (PIB) PET studies of amnestic Alzheimer's disease (AD) have been conducted [2, 3, 5], the link between amyloid-β (Aβ) and regional brain dysfunction remains controversial. However, two PIB studies of PCA supported the possible link between Aβ deposition and clinical features [7, 10]. Here, we describe a patient with PCA who showed left homonymous hemianopsia and uncoupling between PIB uptake and glucose metabolism in the right occipital lobe.

A 63-year-old woman consulted our hospital with a 5-year history of poor vision. She first noticed that characters on posters appeared to be shaking. One year later, she found difficulty in reading subtitles in movies and then she became unable to read books. On neurological examination, she showed left homonymous hemianopsia. A Goldmann dynamic visual field examination demonstrated macular-sparing left homonymous hemianopsia. Visual acuity was normal and bilateral light reflexes were prompt. Other neurological examinations were normal. On neuropsychological evaluations, she showed visuospatial dysfunction and dyscalculia. MMSE score was 26 of 30. Memory function was preserved. She demonstrated disturbed recognition of superimposed figures. Face and color recognition were normal.

Cerebrospinal fluid (CSF) Aβ_{42} was decreased (297 pg/ml) and in normal controls, the levels are 874 $\pm$ 293 pg/ml (mean $\pm$ SD, INNOTEST® β-AMYLOID$_{(1\text{-}42)}$, Innogenetics, Ghent, Belgium). CSF tau protein phosphorylated at serine 199 was increased (1.36 pM). In normal controls, these levels are 0.6 $\pm$ 0.4 pM [4]. [^{18}F] fluorodeoxyglucose (FDG) PET image was acquired for 6 min starting 45 min after the injection of 150 MBq of tracer. The accumulation of [^{11}C] PIB was evaluated by a standardized uptake value ratio (SUVR) on a summing image obtained 40–60 min after injection of 500 MBq of tracer taking the cerebellar cortex as a reference region. [^{18}F] FDG PET showed hypometabolism in the temporo-parieto-occipital lobe predominantly on the right (Fig. 1d–f). [^{11}C] PIB PET demonstrated increased uptake in the bilateral frontal lobes and parietal and occipital cortices with more intense uptake on the right (Fig. 1g–i). In the right occipital lobe, FDG uptake showed lower metabolism in the lateral occipital cortex (Fig. 1d, e, arrow) than in the calcarine cortex (Fig. 1d, e, arrowhead). In contrast, amyloid imaging demonstrated high PIB uptake in the right calcarine cortex (Fig. 1g, h, arrowhead) while the adjacent lateral occipital cortex showed normal PIB uptake (Fig. 1g, h, arrow).

It was shown that macular sparing occurred when the posterior part of the calcarine cortex was spared in patients with striate cortical disease such as infarction, neoplasm and cerebromalacia, while macular splitting occurred when the occipital pole and operculum were involved [6]. Neuroimaging studies of our patient demonstrated that in the occipital lobe, there were two regions showing different

T. Kambe · Y. Motoi (✉) · N. Hattori
Department of Neurology,
Juntendo University School of Medicine,
2-1-1, Hongo Bunkyo-ku, Tokyo 113-8421, Japan
e-mail: motoi@juntendo.ac.jp

K. Ishii
Positron Medical Center,
Tokyo Metropolitan Institute of Gerontology,
1-1 Nakacho, Itabashi, Tokyo 173-0022, Japan

Published online: 14 November 2009

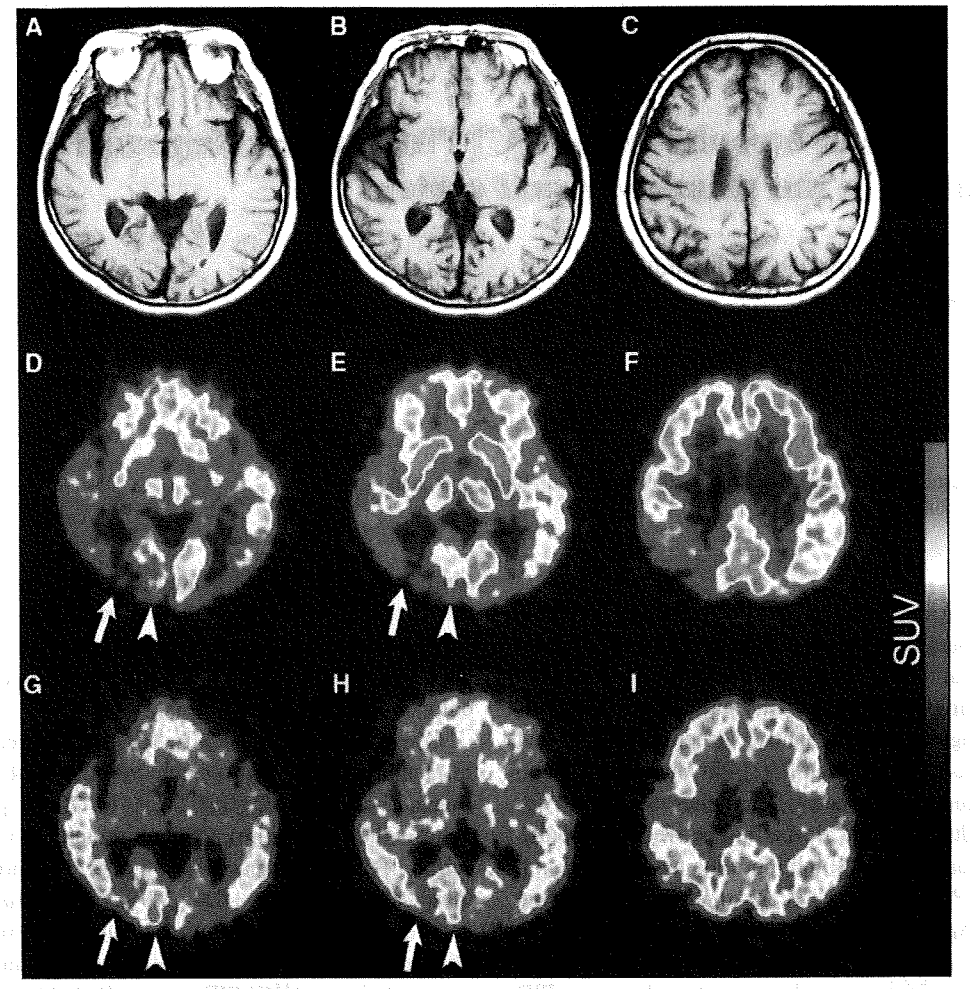

Fig. 1 Transverse T1-weighted MRI sections (**a–c**), PET with [^{18}F] FDG (D-F) and PET with [^{11}C] PIB (**g–i**) of the patient. MRI showed the absence of cerebral infarction and atrophy (**a**). The medial region including the calcarine cortex, (**d, e, g, h** *arrowhead*) showed moderately decreased FDG uptake and very high PIB uptake. In contrast, the lateral region demonstrated severely depressed FDG uptake without remarkable PIB uptake (**d, e, g, h**, *arrow*)

PIB/FDG patterns: a medial region (in the calcarine cortex, Fig. 1d, e, g, h arrowhead) with high PIB uptake and moderately decreased FDG uptake, and a lateral region with normal PIB uptake but severely depressed FDG uptake (Fig. 1d, e, g, h, arrow). Since PIB uptake in the medial region did not spare the occipital pole, we concluded that the lateral region is more likely to have contributed to the macular-sparing left hemianopsia.

We postulate that in the occipital lobe of our patient, Aβ deposition was not associated with the clinical features. Other factors such as neurofibrillary tangles might have contributed to the clinical features [9].

Acknowledgments We are grateful to Dr. Yoko Chikaoka for excellent technique regarding CSF analysis.

References

1. Benson DF, Davis RJ, Snyder BD (1988) Posterior cortical atrophy. Arch Neurol 45:789–793
2. Edison P, Archer HA, Hinz R, Hammers A, Pavese N, Tai YF, Hotton G, Cutler D, Fox N, Kennedy A, Rossor M, Brooks DJ (2007) Amyloid, hypometabolism, and cognition in Alzheimer disease: an [11C]PIB and [18F]FDG PET study. Neurology 68:501–508
3. Frisoni GB, Lorenzi M, Caroli A, Kemppainen N, Nagren K, Rinne JO (2009) In vivo mapping of amyloid toxicity in Alzheimer disease. Neurology 72:1504–1511
4. Itoh N, Arai H, Urakami K, Ishiguro K, Ohno H, Hampel H, Buerger K, Wiltfang J, Otto M, Kretzschmar H, Moeller HJ, Imagawa M, Kohno H, Nakashima K, Kuzuhara S, Sasaki H, Imahori K (2001) Large-scale, multicenter study of cerebrospinal fluid tau protein phosphorylated at serine 199 for the antemortem diagnosis of Alzheimer's disease. Ann Neurol 50:150–156

5. Li Y, Rinne JO, Mosconi L, Pirraglia E, Rusinek H, DeSanti S, Kemppainen N, Nagren K, Kim BC, Tsui W, de Leon MJ (2008) Regional analysis of FDG and PIB-PET images in normal aging, mild cognitive impairment, and Alzheimer's disease. Eur J Nucl Med Mol Imaging 35:2169–2181
6. McFadzean R, Brosnahan D, Hadley D, Mutlukan E (1994) Representation of the visual field in the occipital striate cortex. Br J Ophthalmol 78:185–190
7. Ng SY, Villemagne VL, Masters CL, Rowe CC (2007) Evaluating atypical dementia syndromes using positron emission tomography with carbon 11 labeled Pittsburgh Compound B. Arch Neurol 64:1140–1144
8. Renner JA, Burns JM, Hou CE, McKeel DW Jr, Storandt M, Morris JC (2004) Progressive posterior cortical dysfunction: a clinicopathologic series. Neurology 63:1175–1180
9. Tang-Wai DF, Graff-Radford NR, Boeve BF, Dickson DW, Parisi JE, Crook R, Caselli RJ, Knopman DS, Petersen RC (2004) Clinical, genetic, and neuropathologic characteristics of posterior cortical atrophy. Neurology 63:1168–1174
10. Tenovuo O, Kemppainen N, Aalto S, Nagren K, Rinne JO (2008) Posterior cortical atrophy: a rare form of dementia with in vivo evidence of amyloid-beta accumulation. J Alzheimers Dis 15:351–355

Original article

Nuclear Medicine Communications

Competition between ^{11}C-raclopride and endogenous dopamine in Parkinson's disease

Kenji Ishibashi[a,b], Kenji Ishii[b], Keiichi Oda[b], Hidehiro Mizusawa[a] and Kiichi Ishiwata[b]

Objective The aim of this study was to understand whether the increase in ^{11}C-raclopride binding in the striatum of patients with Parkinson's disease (PD) is associated with the depletion of endogenous dopamine.

Methods Positron emission tomography (PET) scans of the two dopamine D_2 receptor ligands, ^{11}C-raclopride and ^{11}C-*N*-methylspiperone (^{11}C-NMSP), and the dopamine transporter ligand, ^{11}C-2β-carbomethoxy-3β-(4-fluorophenyl)-tropane, were performed on five patients with PD and seven controls. The binding of each tracer was calculated by using a (region–cerebellum)/cerebellum ratio in the caudate, anterior putamen, and posterior putamen.

Results In patients with PD, the ^{11}C-raclopride to ^{11}C-NMSP ratios in the posterior putamen, which was the subregion of the striatum with the lowest binding of ^{11}C-2β-carbomethoxy-3β-(4-fluorophenyl)-tropane, were the largest among all three subregions of the striatum. In controls, the ^{11}C-raclopride to ^{11}C-NMSP ratios in all three subregions of the striatum were within a constant range.

Conclusion In patients with PD, the kinetic difference between ^{11}C-raclopride and ^{11}C-NMSP was found prominently in the posterior putamen, in which presynaptic degeneration occurred most profoundly. Therefore, we concluded that the increase in ^{11}C-raclopride binding in the striatum of patients with PD was strongly associated with the depletion of endogenous dopamine. ^{11}C-NMSP can be chosen in the place of ^{11}C-raclopride in cases in which it may be essential to eliminate the influence of endogenous dopamine. *Nucl Med Commun* 00:000–000 © 2010 Wolters Kluwer Health | Lippincott Williams & Wilkins.

Nuclear Medicine Communications 2010, 00:000–000

Keywords: ^{11}C-2β-carbomethoxy-3β-(4-fluorophenyl)-tropane, ^{11}C-*N*-methylspiperone, ^{11}C-raclopride, endogenous dopamine, Parkinson's disease, positron emission tomography

[a]Department of Neurology and Neurological Science, Graduate School, Tokyo Medical and Dental University and [b]Positron Medical Center, Tokyo Metropolitan Institute of Gerontology, Tokyo, Japan

Correspondence to Kiichi Ishiwata, MD, Positron Medical Center, Tokyo Metropolitan Institute of Gerontology, 1-1 Nakacho, Itabashi-ku, Tokyo 173-0022, Japan
Tel: +81 3 3964 3241; fax: +81 3 3964 2188; e-mail: ishiwata@pet.tmig.or.jp

Received 9 September 2009 **Revised** 5 October 2009
Accepted 6 October 2009

Introduction

Among positron emission tomography (PET) radioligands for mapping postsynaptic dopamine D_2 receptors (D_2Rs) in the striatum, carbon-11-labeled raclopride is most often used as a standard D_2R ligand because of its high selectivity [1,2]. We have reported the coupling of age-related decline in postsynaptic D_2Rs and presynaptic dopamine transporters (DATs) in the striatum of normal individuals by using PET with ^{11}C-raclopride and ^{11}C-2β-carbomethoxy-3β-(4-fluorophenyl)-tropane (^{11}C-CFT), respectively [3]. The binding of the two tracers correlated well, irrespective of age. In contrast, our preliminary findings revealed that compared with the binding of ^{11}C-raclopride, the binding of ^{11}C-*N*-methylspiperone (^{11}C-NMSP), another radioligand for mapping D_2Rs, correlates more strongly with that of ^{11}C-CFT in normal individuals (unpublished data). The difference between the two D_2R ligands, ^{11}C-raclopride and ^{11}C-NMSP, can be explained by the variable binding of ^{11}C-raclopride in response to changes in the concentrations of endogenous dopamine caused by various physiological factors. The above concept is based on the following findings: (i) several studies with ^{3}H-labeled ligands explain the differences in the in-vivo binding properties of the two D_2R ligands [4–9]. Specifically, the binding of ^{11}C-raclopride to the D_2Rs in the striatum is reversible in the time frame of a PET scan and competitive with that of endogenous dopamine. In contrast, the binding of ^{11}C-NMSP is substantially irreversible in the time frame of a PET scan and not competitive with that of endogenous dopamine. Consequently, the binding of ^{11}C-raclopride is affected by the concentration of endogenous dopamine, whereas that of ^{11}C-NMSP is not; (ii) considerable interindividual and intraindividual variabilities in the concentration of endogenous dopamine in individuals with normal nigrostriatal dopaminergic function has been reported in earlier studies on the measurements of dopamine metabolites in cerebrospinal fluid [10–12].

On the basis of the above findings, the binding of ^{11}C-raclopride could be relatively higher than that of ^{11}C-NMSP in the striatum of patients with PD, on account of the depletion of endogenous dopamine and preserved D_2Rs in the striatum [13–15]. Moreover, the differences

0143-3636 © 2010 Wolters Kluwer Health | Lippincott Williams & Wilkins

DOI: 10.1097/MNM.0b013e328333e3cb

in the binding levels of the two D_2R ligands among the different subregions of the striatum could be greater in the following order: the posterior putamen > anterior putamen > caudate, corresponding to the reported order of the extent of presynaptic degeneration [16–20]. However, contrary to these considerations, Kaasinen *et al.* [21] reported that the increased binding of ^{11}C-raclopride in patients with PD did not result from the reduction in the amount of endogenous dopamine, but from the upregulation of the D_2Rs. Their conclusion is questionable in light of the binding properties of radioligands described above [4–9] and earlier reports on morphological studies, which state that parkinsonian symptoms appear when 80% of the striatal dopamine is lost [15].

The aim of this study was to understand whether the increase in ^{11}C-raclopride binding in the striatum of patients with PD is associated with the depletion of endogenous dopamine. For this purpose, we performed both ^{11}C-raclopride and ^{11}C-NMSP PET scans on patients with PD and the differences in the binding of the two radioligands were evaluated, particularly in the subregions of the striatum, in relation to the presynaptic functionality evaluated with the binding of ^{11}C-CFT. To confirm the reliability of this study, we performed region of interest (ROI) analysis by using anatomical standardization and coregistration of the images, as objectively as possible.

Materials and methods

Participants

A total of 27 individuals (five patients with PD and 22 healthy volunteers) participated in this retrospective study. We divided the 22 healthy volunteers into three groups (first group: seven, second group: eight, third group: seven), and the five patients with PD were classified into the third group. In the first group, seven volunteers [four men and three women; age, 55–68 years (mean=60.6, SD=5.4)] underwent static PET scans of ^{11}C-raclopride to create the ^{11}C-raclopride template. In the second group, eight volunteers [8 men; age, 20–22 years (mean=20.6, SD=0.7)] underwent dynamic PET scans of ^{11}C-NMSP to ascertain the method for static PET scans that represent ^{11}C-NMSP binding to the D_2Rs, as we had earlier validated static PET scans for both ^{11}C-raclopride and ^{11}C-CFT [3,22]. In the third group, five patients with PD [two men and three women; age, 53–67 years (mean=57.8, SD=5.5)] and seven volunteers [7 men; age, 21–23 years (mean=22.3, SD=1.0)] underwent three static PET scans of ^{11}C-raclopride, ^{11}C-NMSP, and ^{11}C-CFT. A magnetic resonance imaging (MRI) scan of the brain was performed on all participants to check for the abnormal lesion. All volunteers were defined as healthy on the basis of their medical history, the results of their physical and neurological examination performed by neurologists, and the findings of the MRI that were reported by the radiologists. None of the volunteers was on any medication at the time of this study. All patients were drug naive at the time of the study. Table 1 shows the demographic data of the patients. This study protocol was approved by the Ethics Committee of the Tokyo Metropolitan Institute of Gerontology. Written informed consent was obtained from all participants of this study.

Table 1 Clinical features of patients with Parkinson's disease

Patient	Sex	Age (years)	Duration (years)	Side[a]	Hoehn–Yahr stage	Symptoms
1	F	54	2	Right	1	Tremor, rigidity
2	F	57	1	Right	1	Tremor
3	M	67	5	Right	2	Tremor, rigidity
4	M	58	1	Right	1	Tremor
5	F	53	2	Left	1	Tremor

F, female; M, male.
[a]Affected side.

Positron emission tomography imaging

PET imaging was performed at the Positron Medical Center, Tokyo Metropolitan Institute of Gerontology by using a SET-2400W scanner (Shimadzu, Kyoto, Japan) in the three-dimensional scanning mode for static scans or the two-dimensional scanning mode for dynamic scans. The transmission data were acquired by using a rotating ^{68}Ga/^{68}Ge rod as a source for attenuation correction. Images with 50 slices were obtained with a resolution of $2 \times 2 \times 3.125$ mm voxels and a 128×128 matrix. ^{11}C-raclopride, ^{11}C-NMSP, and ^{11}C-CFT were prepared by the reaction of ^{11}C-methyl triflate and the respective desmethyl compound as described in earlier studies [23,24].

Dynamic scanning of ^{11}C-NMSP was performed for 90 min after an intravenous bolus injection of 640 ± 67 MBq (mean ± SD). The specific activity ranged from 29.2 to 109.3 GBq/μmol. Static scannings of the three tracers were performed for 40–55, 54–66, and 75–90 min after intravenous bolus injection of ^{11}C-raclopride, ^{11}C-NMSP, and ^{11}C-CFT, respectively. Two PET studies with ^{11}C-raclopride and ^{11}C-CFT were carried out at an interval of 2.5–3 h on the same day, and the study with ^{11}C-NMSP was carried out on another day. The injection doses (mean ± SD) for ^{11}C-raclopride, ^{11}C-NMSP, and ^{11}C-CFT were 298 ± 60, 321 ± 14, and 331 ± 22 MBq, respectively, and the specific activities were 14.0–95.9, 14.5–82.4, and 14.5–68.0 GBq/μmol, respectively, at the time of injection.

Magnetic resonance imaging

The MRI scans were performed at the Tokyo Metropolitan Geriatric Hospital. Transaxial T1-weighted images (three-dimensional spoiled-gradient-recalled echo images; repetition time = 9.2 ms, echo time = 2.0 ms, matrix size = $256 \times 256 \times 124$, voxel size = $0.94 \times 0.94 \times 1.3$ mm) and transaxial T2-weighted images (first spin echo; repetition time = 3000 ms, echo time = 100 ms, matrix size = $256 \times 256 \times 20$, voxel size = $0.7 \times 0.7 \times 6.5$ mm) were obtained by using a 1.5-Tesla Signa EXCITE HD scanner (GE, Milwaukee, Wisconsin, USA).

Analysis of positron emission tomography images

Image manipulations were performed using Dr View version R2.0 (AJS, Tokyo, Japan) and statistical parametric mapping 2 (SPM2; Functional Imaging Laboratory, London, UK) implemented in MATLAB version 7.0.1 (The MathWorks, Natick, Massachusetts, USA). We used SPM2 for the anatomical standardization and coregistration of the obtained images. To eliminate arbitrariness and subjectivity, both of which are disadvantages of conventional ROI analysis in which ROIs are placed individually, and to improve objectivity, we placed ROIs on the same anatomical position for all participants at a time by standardization of each image, as described below.

Creation of the ^{11}C-raclopride template and average MRI image

The ^{11}C-raclopride template, which was used as the standard for brain images in this study, was created from the integral ^{11}C-raclopride images taken from the seven healthy individuals of the first group, as described earlier [25,26]. For this purpose, MRI-based spatial normalization was used. First, individual ^{11}C-raclopride images were coregistered with their corresponding T1-weighted MRI images. Next, individual MRI images were spatially transformed to the SPM2-T1-MRI template. The same deformation parameters were applied to the individual coregistered ^{11}C-raclopride images. Finally, the ^{11}C-raclopride template was made by averaging the transformed ^{11}C-raclopride images of seven healthy individuals and applying a smoothing Gaussian filter (full width at half maximum=8 × 8 × 8 mm). In addition, we obtained the average MRI image by averaging the transformed MRI images of seven healthy individuals.

Creation of normalized images of ^{11}C-raclopride, ^{11}C-NMSP, and ^{11}C-CFT

Individual ^{11}C-raclopride, ^{11}C-NMSP, and ^{11}C-CFT PET images were coregistered. Next, the individual ^{11}C-raclopride images were anatomically normalized to the standard brain images by using the ^{11}C-raclopride template described above which was developed in-house. The same deformation parameters were applied to the individual coregistered ^{11}C-NMSP and ^{11}C-CFT images. Subsequently, we obtained the individual normalized PET images of ^{11}C-raclopride, ^{11}C-NMSP, and ^{11}C-CFT. All the normalized PET images and the average MRI image were anatomically the same.

Uptake ratio index of ^{11}C-raclopride, ^{11}C-NMSP, and ^{11}C-CFT

We placed the ROIs on the average MRI image: one ROI with an 8-mm diameter was placed on the caudate, one ROI with an 8-mm diameter on the anterior putamen, and one ROI with an 8-mm diameter on the posterior putamen on both sides in each of five contiguous slices. A total of 30 ROIs with 10-mm diameter were placed throughout the cerebellar cortex in three contiguous slices. These ROIs placed on the average MRI were spatially moved on each normalized PET image.

To evaluate the binding of ^{11}C-raclopride, ^{11}C-NMSP, and ^{11}C-CFT to their respective binding sites, we calculated the uptake ratio index (URI) by the following formula [18,27]: URI=[(activity in each region) − (activity in the cerebellum)]/[(activity in the cerebellum)]. Earlier, we had validated the use of the URI as a method to estimate the binding potential of ^{11}C-raclopride and ^{11}C-CFT [3,22].

The following two analysis methods were performed. First, we compared the three tracers in both patients with PD and healthy volunteers, using the URI of every ROI placed on the striatum. Second is the comparison of the ipsilateral and contralateral sides to the predominant symptoms in patients with PD.

Relationship between binding of ^{11}C-NMSP to D_2Rs and uptake ratio index

To validate the use of the URI for ^{11}C-NMSP, we examined the correlation between the binding of ^{11}C-NMSP to the D_2Rs (association constant, k_3) and the URI in eight healthy volunteers of the second group. Six ROIs were placed on the striatum of each dynamic scanned participant. The k_3 was estimated by graphical analysis of irreversible ligands, using the cerebellum as a reference [28,29]. The cerebellum was selected as a reference region in the analysis because the density of D_2Rs and serotonin 5-HT$_2$ receptors in this region is negligible. The URI of each ROI was also estimated, as described above. Next, we compared the k_3 values of total 48 ROIs with the URI.

Statistics

The differences in averages and variances were tested by Student's *t*-test and one-way analysis of variance, respectively. Correlations between the two groups were assessed by linear regression analysis with Pearson's correlation test. *P* values less than 0.01 were considered statistically significant.

Results

There was a significant positive linear correlation between k_3 and the URI of ^{11}C-NMSP (r=0.98; $P < 0.0001$), as shown in Fig. 1. Therefore, the URI was adopted for further analyses.

In normal individuals (Fig. 2), the URI of ^{11}C-raclopride correlated significantly with that of ^{11}C-CFT in the posterior putamen, but not in the other two subregions. Conversely, the URI of ^{11}C-NMSP correlated significantly with that of ^{11}C-CFT in all three subregions.

In patients with PD (Fig. 3), a negative correlation (r=0.71; $P < 0.0001$) was found between the URI of